ELSEVIER

Synthetic Metals 114 (2000) 201–207

SYNTHETIC METALS

www.elsevier.com/locate/synmet

Photosensitization of ITO and nanocrystalline TiO_2 electrode with a hemicyanine derivative

Zhongsheng Wang [a], Yanyi Huang [a], Chunhui Huang [a,*], Jie Zheng [a], Humin Cheng [b], Shujian Tian [b]

[a] *State Key Laboratory of Rare Earth Materials Chemistry and Applications, Peking University–The Hong Kong University Joint Laboratory in Rare Earth Materials and Bioinorganic Chemistry, Peking University, Beijing 100871, People's Republic of China*

[b] *College of Chemistry & Molecular Engineering, Peking University, Beijing 100871, People's Republic of China*

Received 8 September 1999; received in revised form 23 March 2000; accepted 31 March 2000

Abstract

The monochromophore (*E*)-*N*-Hexadecyl-4-(2-(4-diethylamino)phenyl)ethenyl) pyridinium stearate was synthesized. The LB film of the dye-modified ITO gives rise to cathodic photocurrent, while the dye-sensitized nanocrystalline TiO_2 film generates anodic photocurrent. Having investigated some factors such as electron donor and acceptor, and bias voltage that may affect the magnitude of photocurrent and the direction of current flow, we proposed a mechanismic model for photocurrent generation. The quantum yield is about 0.2% for monolayer LB film-modified ITO electrode and 1.0% for the dye-sensitized nanocrystalline TiO_2 film under irradiation of 469-nm light in 0.1 M KCl aqueous solution without applied potential. Under 100 mW/cm^2 illumination of simulated solar light, the dye-sensitized nanocrystalline TiO_2 film generated greater than 1 mA/cm^2 of current density, which is comparatively high among the organic dyes.

Keywords: Photoelectric conversion; Hemicyanine; Sensitization; Nanoparticle; TiO_2

1. Introduction

Considerable attention has been directed towards dye-sensitized nanocrystalline semiconductor films [1–7] since O'Regen and Grätzel reported a high-efficiency dye-sensitized solar cell [8]. Nanocrystalline semiconductor films are highly porous, thus having a large internal surface area. Only the first monolayer of adsorbed dye results in efficient electron injection into the semiconductor, but the light-harvesting efficiency of a single dye monolayer is very small. In a mesoporous film consisting of nanometer-sized TiO_2 particles, the effective surface area can be enhanced about 1000-fold theoretically, thus making light absorption efficient even with only a dye monolayer on each particle.

Recent work on dye-sensitized solar cell is centered on ruthennium–bipyridine complexes [9–11] sensitizing nanocrystalline TiO_2 films, which has been proven to be highly efficient in photon-to-electron conversion. However, in order to study photoelectric conversion mechanism and develop a more efficient dye-sensitized solar cell, it is necessary to probe the sensitization of other kinds of dyes, such as organic molecules, which are easy to be modified.

Our group has been systematically studying the second order nonlinear optical properties (NLO) and the photoelectric characteristics of hemicyanine derivatives [12–16]. We have found that hemicyanine system, which has good NLO property, usually possesses good photoelectric conversion property. The principle of second-harmonic nonlinear optics requires that the molecule have a large difference of the dipole moment between the ground and excited states, and the molecule usually requires asymmetric structure, that is, a strong donor in one side and a strong acceptor in another side linking with a π bridge usually leads to large SHG effect. On the other hand, photocurrent generation is associated with the charge separation process, which also requires a large dipole moment in the excited state. Therefore, it is rational to build a correlation between second-harmonic nonlinear optics and photocurrent generation for hemicyanine dyes. In order to understand

* Corresponding author. Tel.: +86-10-6275-7156; fax: +86-10-6275-1708.

E-mail address: hch@chemms.chem.pku.edu.cn (C. Huang).

0379-6779/00/$ - see front matter
PII: S0379-6779(00)00261-7

and compare the photoelectric characteristics of the dyes on ITO and TiO_2 surfaces, here we report the photocurrent generation from an amphiphilic monochromophore stilbazolium LB film-modified ITO electrode and from the same dye-sensitized nanocrystalline TiO_2 electrode.

2. Experimental section

2.1. Materials

(*E*)-*N*-Hexadecyl-4-(2-(4-(diethylamino)phenyl)ethenyl)pyridinium iodide (PI) was synthesized according to the literature [17], then the stilbazolium stearate (hereafter denoted as PS and the structural formula is shown in Scheme 1) was prepared from PI with ion-exchange method. The product (orange color) was purified by column chromatography on silica gel with chloroform as eluant. mp, 79–81°C. The purity was identified by ^1H NMR (400 MHz, $CDCl_3$, ppm): $\delta = 0.88$ (t, 6H, $2CH_3$), 1.25 (m, 60 H, $27CH_2$, $2CH_3$), 1.61 (m, 2H, CH_2), 1.90 (m, 2H, CH_2), 2.29 (t, 2H, CH_2–COO^-), 3.42 (m, 4H, $N(CH_2)_2$), 4.54 (t, 2H, N^+–CH_2), 6.65 (d, 2H, phenyl), 6.78 (d, 1H, CH═), 7.48 (d, 2H, phenyl), 7.58 (d, 1H, CH═), 7.82 (d, 2H, pyridyl), 8.80 (d, 2H, pyridyl). The 1592 cm^{-1} peak in its IR spectrum can be assigned to the $RCOO^-$ group, which indicates that the ion exchange is successful.

Methyl viologen was synthesized according to the reference [18], and ^1H NMR confirmed the purity. All other chemicals were reagent grade and were used without further purification.

2.2. Preparation of nanocrystalline TiO_2 films

Nanocrystalline TiO_2 films were prepared through spin-coating a viscous dispersion of colloidal TiO_2 particles on a conducting glass (STN, ITO glass, indium-doped SnO_2 overlayer, transmission > 90% in the visible region, sheet resistance 60 Ω/square) followed by heating under air for 30 min at 400°C. Two pieces of Scotch (3M) adhesive tapes (about 40-μm thick) were applied to the face of the conductive glass plate to mask two strips for electric contact. Three-micrometer-thick colloidal TiO_2 film can be prepared by repeating the above procedure, and the thickness was controlled by profilometry (DEKTAK 3). The sheet resistance of ITO after sintering at 400°C for 30 min or longer is about 500 Ω/square. TiO_2 colloidal solution was prepared by hydrolysis of titanium tetraisopropoxide (ACROS) in a similar procedure described in the literature [19], except that 25% Carbowax M-20,000 by weight of TiO_2 was added to the colloidal solution. The size of the colloidal particles was ca. 8nm determined by TEM (JEOL-200cx), and X-ray diffraction analysis of the membrane of TiO_2 showed that they crystallized in complete anatase. The high resolution scanning electron microscopy (AMRAY 1910FE FIELD EMISSION MICROSCOPE) reveals the TiO_2 film to be composed of a three-dimensional network of interconnected particles that have an average size of approximately 10 nm. Obviously, the sintering at 400°C only induced a slight growth of particles.

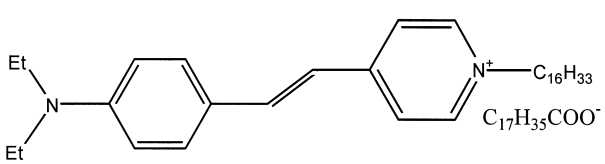

Scheme 1. Structural formula of PS.

Coating of the TiO_2 surface with the dye was carried out by soaking the film for 24 h in a 3×10^{-4} M solution of the dye in chloroform. In order to avoid rehydration of the TiO_2 surface or capillary condensation of water vapor from ambient air inside the nanopores of the film, the electrode was dipped into the dye solution while it was still hot, namely, its temperature was about 80°C. After completion of the dye adsorption, the electrode was washed with dry ethanol, dried in a stream of nitrogen, and immediately wetted with electrolyte for testing.

2.3. LB film preparation

Solution of the dye in chloroform was spread dropwise onto a clean water subphase, which was prepurified by passing through an Easy Pure RF Compact Ultrapure Water system (Barastead, USA), by syringe at a subphase temperature of 20 ± 1°C. Chloroform was allowed to evaporate for 15 min, and the floating film was then compressed at a rate of 40 cm^2/min. Before LB film deposition, ITO glass was soaked in a saturated solution of CH_3ONa in CH_3OH for 24 h. Thereafter, it was ultrasonically washed in ethanol, acetone and ultrapure water successively. The surface pressure–area (π–A) isotherm was recorded (Fig. 1). The limiting area per molecule, obtained through extrapolation of the rising portion of the isotherms to $\pi = 0$, was 75 $Å^2$/molecule. The monolayer was deposited onto the ITO substrate at a rate of 4 mm/min (vertical dipping) under a constant surface pressure of 30 mN/m. The transfer ratios were ca. 1.0 ± 0.1.

2.4. Photocurrent measurements

The photocurrent–potential characteristics were measured using a xenon arc light source and a model 600 voltammetric analyzer (CH Instruments, USA). The photocurrent action spectrum was obtained with a series of filters (Toshiba, Japan) with certain band passes. The monochromatic photon flux impinging on the cell was determined by an EG&G PARC Model 550 radiometer (USA). The electrochemical system employed is a single-

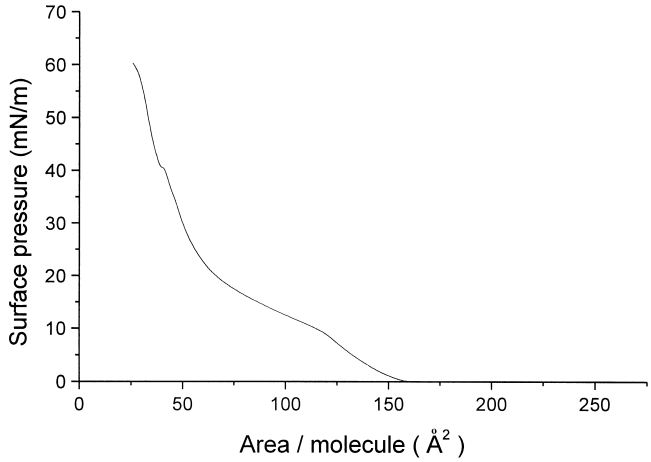

Fig. 1. Surface pressure–area (π–A) isotherm of the dye at the air/water interface (20 ± 1°C).

compartment, three-electrode cell having a flat window with a 0.20 cm^2 effective area for illumination. The counter electrode was a polished platinum wire, and the reference was a saturated calomel electrode (SCE). All potentials are reported against SCE. The supporting electrolyte was an aqueous solution of 0.1 M KCl or 0.1 M tetrabutylammonium iodide + 0.01 M I_2 in propylene carbonate (ACROS).

2.5. Instrumentation

^{1}H NMR spectrum was recorded on a Brucker ARX 400. The IR spectrum was recorded on a Nicolet 7199B FT-IR spectrometer. Electronic spectra were measured with a Shimadzu model 3100 UV–vis–NIR spectrophotometer. LB film-modified ITO electrodes were fabricated using a model 622 NIMA Langmuir–Blodgett Trough.

3. Results and discussion

3.1. Absorption characteristics of LB films and dye-sensitized TiO_2 films

UV–vis absorption spectra for the dye LB film on ITO, the dye adsorbed on TiO_2 film and the solution of the dye in chloroform are all shown in Fig. 2. It can be seen that the maximum absorption peaks appear at $\sim$470 and $\sim$450 nm for the dye in LB film and on TiO_2 film, respectively, which are blue-shifted by 30 and 50 nm, respectively, with respect to the maximum peak for the dye in chloroform solution. This indicates H-aggregates are formed in both cases. The absorbance of the dye-loaded TiO_2 film at 450 nm is 0.8, which is much greater than that of the dye on ITO glass (0.008 at 470 nm). Absorbance of 0.8 divided by the extinction coefficient of the dye ($\varepsilon = 3.57 \times 10^7$ cm^2 mol^{-1}) yields the surface concentration of the dye, 2.24×10^{-8} mol cm^{-2}. As each dye molecule occupies an area of 0.75 nm^2, assuming complete monolayer coverage, the inner surface of the TiO_2 film is 100 cm^2 for each 1 cm^2 of geometric surface. Thus, the roughness factor is 100, which is smaller than the expected value of 1000 for 3-μm-thick TiO_2 films [19]. The difference is possibly ascribed to the necking between adjacent particles of TiO_2 [8] and the blocking of the dye with long hydrophobic chain when they are passing through the pores.

3.2. Photocurrent generation

In 0.1 M KCl aqueous solution, a steady cathodic photocurrent was obtained from the LB film-modified ITO electrode when it was illuminated by white light or by monochromatic light under the condition of zero bias voltage (vs. SCE). However, we observed a steady anodic photocurrent when the dye was loaded on the nanocrystalline TiO_2 film. While Fig. 3 shows the action spectrum and absorption spectrum for the dye monolayer LB film-modified ITO, respectively, Fig. 4 shows both spectra for the dye-sensitized TiO_2 film. In both cases, the action spectrum matches its related absorption spectrum, indicating that the dye is responsible for the photocurrent genera-

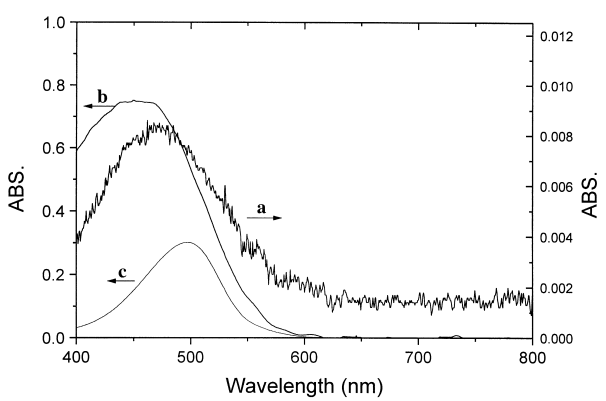

Fig. 2. UV–vis spectra for the dye LB film on one side of ITO (a), the dye adsorbed on TiO_2 film (b), and solution of the dye in chloroform (c), respectively.

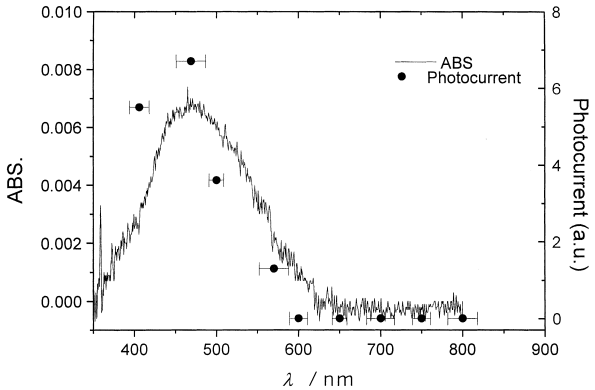

Fig. 3. Photocurrent action spectrum (full circle with error bars, 0.1 M KCl as electrolyte solution, pH 5.6) and absorption spectrum (solid line) for the dye monolayer on ITO electrode under zero bias voltage (vs. SCE). The intensities of different monochromatic light are all normalized for all action spectra.

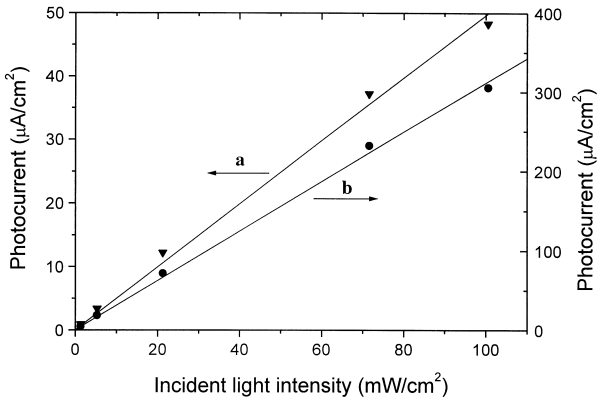

Fig. 5. Relationship between incident light intensities and photocurrents for the dye-sensitized TiO_2 film. A 420-nm cut-off filter was used to avoid light excitation of the semiconductor: (a) in 0.1 M KCl aqueous solution (down full triangle); (b) in 0.1 M $Bu_4NI + 0.01$ M I_2 in propylene carbonate (full circle).

tion. The quantum yield is about 0.2% for the dye LB film, and 1.0% for the dye-sensitized TiO_2 film under 1.69 mW/cm^2 irradiation of 469-nm light without applied potential in 0.1 M KCl aqueous solution. The latter is five times as large as the former, implying that charge separation in the dye-sensitized TiO_2 film is easier than in the dye LB film-modified ITO electrode and that the electrons and holes transfer faster in the former than in the latter. Although the conduction band of SnO_2 is lower than that of TiO_2, the latter is more favorable for electron injection. We can see from the results that electron transfer can take place either from the excited state of the dye to the conduction band of nanostructured TiO_2 or from the conduction band of ITO to the dye. The photocurrent resulted from the dye is directly proportional to the incident light intensity (Fig. 5), which represents unimolecule recombination process [20] for the charge separation both in LB film and in dye-loaded TiO_2 film.

3.3. Potential dependence of electron injection

Charge separation is the key factor for photocurrent generation, so high photocurrent is usually based on efficient charge separation. Fig. 6 shows photocurrent–potential plots for the dye-loaded TiO_2 electrodes in solutions containing iodide or hydroquinone as an electron donor. The photocurrent onsets are -0.42 V for the iodide-containing solution and -0.38 V for the hydroquinone-containing solution, respectively, which are close to the flatband potential of the TiO_2 electrode that is -0.52 V at pH 3 [19]. Thereafter, the photocurrents rise steeply and level off at 0 V for the iodide-containing solution and at 0.1 V for the hydroquinone-containing solution, respectively. This result implies that small band bending ($\sim$ 400 mV) within the depletion layer suffices to afford complete charge separation. The result is in agreement with that for Ru–bipyridine-sensitized TiO_2 film [21], and it is under-

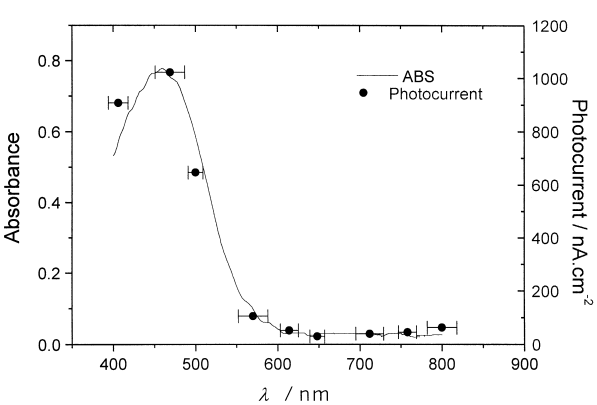

Fig. 4. Photocurrent action spectrum (full circle with error bars, normalized, 0.1 M KCl as electrolyte solution, pH 5.6) and absorption spectrum (solid line) for the dye-sensitized TiO_2 film.

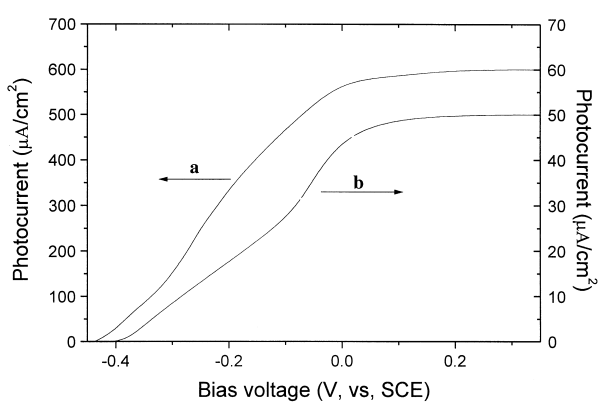

Fig. 6. Photocurrent-applied potential curve recorded under 30.5 mW/cm^2 white light irradiation of the dye-coated TiO_2 film in (a) 0.1 M $Bu_4NI +$ 0.01 M I_2 in propylene carbonate; (b) 0.1 M hydroquinone + 0.1 M KCl aqueous solution.

standable with respect to nanostructured TiO_2 film [22]. The defects and surface states that present at the semiconductor–solution interface are expected to act as recombination centers. However, one can see from the steep edge and rapid attainment of saturation of the photocurrent–potential characteristic curve that this is not the case. Now that the charge separation is very efficient from Fig. 6, why are the photocurrents so low, compared with Ru(II)–bipyridine complex-sensitized TiO_2 electrode? This may be ascribed to the short lifetime of the excited state of the dye ($\sim 10^1$ ps), because the higher lifetime the excited state of the dye, the higher efficiency the electron injection.

A linear relationship between the observed photocurrent and the bias voltage is shown in Fig. 7 when the applied bias voltage, added to the dye LB film-modified ITO electrode, lies within the range from -150 to 100 mV. With the increase of negative potential, the cathodic photocurrent increases, while with the increase of positive potential, the cathodic photocurrent decreases so much that the direction of current flow is inverted, namely, the cathodic photocurrent changing into anodic photocurrent, when the bias voltage exceeds 50 mV.

3.4. Effect of electron donors

In 0.1 M KCl without any electron donor, only ~ 4 $\mu A/cm^2$ photocurrent was obtained under 1.69 mW/cm^2 irradiation of 469-nm light , but when H_2Q was added to the above solution, the photocurrents increased with the increasing of H_2Q in concentration, and attained saturation at ~ 0.04 mM H_2Q (Fig. 8), which corresponds to ~ 9 $\mu A/cm^2$ of photocurrent. Substituting 0.1 M Bu_4NI + 0.01 M I_2 in propylene carbonate for 0.1 M KCl + 0.1 mM H_2Q aqueous solution, we obtained 20 $\mu A/cm^2$ of photocurrent at 469 nm, which is five times as large as that in 0.1 M KCl aqueous solution. This result shows that the addition of electron donor to the solution is advantageous

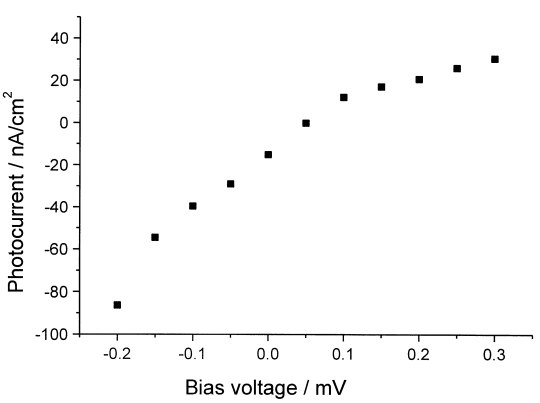

Fig. 7. Photocurrent-applied potential curve recorded under 1.69 mW/cm^2 irradiation of 469-nm light of the dye LB film-modified ITO electrode in 0.1 M KCl aqueous solution. '−' stands for cathodic current; '+' stands for anodic current (the same below).

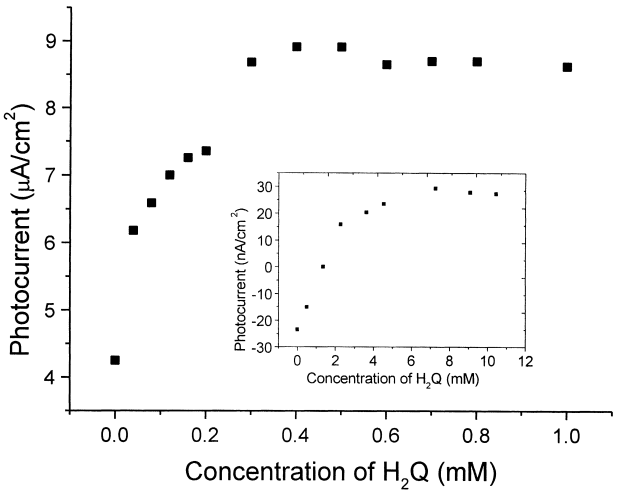

Fig. 8. The dependence of the photocurrents on concentration of H_2Q for the dye-loaded TiO_2 electrode in 0.1 M KCl aqueous solution under 1.69 mW/cm^2 irradiation of 469-nm light at zero bias voltage (vs. SCE); inset is for the LB film-modified ITO electrode under the same condition as above.

to the photocurrent generation, and that a different donor will result in positive effect on photocurrent in varying extent. As we know, donors (such as H_2Q) are favorable for anodic photocurrent but unfavorable for cathodic photocurrent, while acceptors (such as MV^{2+}) are favorable for cathodic current but unfavorable for anodic current [11]. Strangely, when MV^{2+} was added by increment to 0.1 M KCl solution, the photocurrent for dye TiO_2 film had an unobvious change that one can neglect its effect. This result shows that when the dye adsorbed to the TiO_2 film, electron can transfer from the dye so easily to the conduction band of TiO_2 that MV^{2+} can hardly affect the photocurrent.

The inset in Fig. 8 shows the effect of H_2Q concentration on the photocurrent generated by the dye LB film-modified ITO electrode, which is similar to Fig. 8. We can see from this curve that H_2Q can significantly prohibit the cathodic photocurrent generation, and that when the concentration of H_2Q exceeds 2 mM, the current flow can change from cathodic photocurrent to anodic photocurrent. The platform of this curve shows that when the concentration of H_2Q is greater than 5 mM, the anodic photocurrent remains almost constant in the range of H_2Q concentration studied.

Comparing the effect of H_2Q concentration on the anodic and cathodic photocurrent and using the results reported earlier [15,16] as references, we can conclude that the lower the photocurrent, the more significant the effect of H_2Q concentration on photocurrent.

3.5. Mechanismic model for photocurrent generation

Scheme 2 shows the possible mechanism for cathodic and anodic photocurrent generation. The relative positions

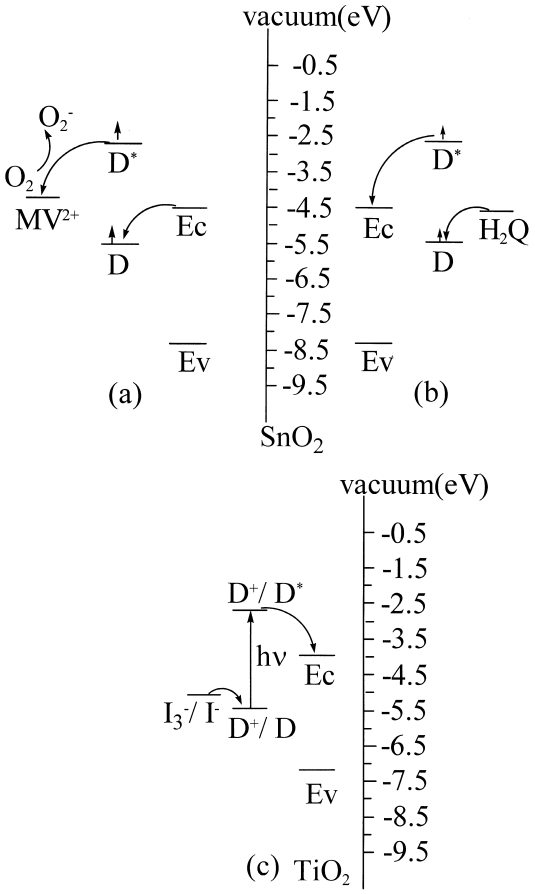

Scheme 2. Schematic presentation for the electron transfer processes. Electron transfer processes for cathodic current generation (a); anodic current generation for the ITO/dye electrode (b), and anodic current generation for the dye coated TiO_2 electrode(c).

of energy levels are determined on the basis of the redox potential of the dye [18], the excitation light energy, vacuum energy levels of the bottom of the conduction band and the top of the valence band [23,24]. On the occasion of LB film on ITO, after the dye molecules are excited from the ground state to the excited state under illumination, the excited dye may either inject electrons into the conduction band of ITO or give electrons to electron acceptor such as O_2 or MV^{2+}. The fact of the cathodic photocurrent generation indicates that electrons may flow from the excited dye to acceptors, and, to complete the circuit, the dye must be regenerated by electron transfer from the conduction band of ITO to the hole residing in the ground state of the dye [24]. Consequently, the cathodic photocurrent is produced. When strong electron donors, such as H_2Q, exists in the system, the quenching of the excited dye becomes energetically favorable. As soon as H_2Q donates electrons to the hole of the ground state dye [16,24], an anion radical of the dye is formed as a result of the energy-transfer quenching and the electron transfer from the conduction band is restrained. The generated anion radical can transfer an electron to the conduction band of ITO, which reduces the cathodic photocurrent, sometimes reversing the current flow direction, or enhances the anodic photocurrent. As for the dye-sensitized TiO_2 film, since the energy level of the dye matches well the energy of the conduction band of the semiconductor, the dye injects an electron to the conduction band of TiO_2 [22] once excited by light, resulting in anodic photocurrent. The explanation for H_2Q enhancing anodic photocurrent also holds for the case in the dye-sensitized TiO_2 film. Although MV^{2+} can decrease the anodic photocurrent resulted from LB film, it has a minor effect on the photocurrent produced by the dye-sensitized TiO_2 film for the abovementioned reason.

4. Conclusion

High-quality LB films of a new hemicyanine derivative with two long alkyl chains were deposited onto the conducting glasses, exhibiting good photoelectric responses. Meanwhile, the dye can adsorb onto the nanometer-sized TiO_2 film, and its photoelectric responses are much better than those for the LB film-modified ITO both in magnitude of photocurrents and in photon-to-electron conversion quantum yield. When nanostructured TiO_2 film was sensitized by the dye, the photocurrent onset extended to 800 nm. Under the illumination of 100 mW/cm^2 simulated solar light, greater than 1 mA/cm^2 photocurrent was obtained with the dye-loaded nanocrystalline TiO_2 electrode, which is a very high value among pure organic dye sensitizers. In order to clarify the processes for electron transfer, we investigated some factors that may affect photocurrent generation and proposed a possible mechanismic model.

Acknowledgements

The authors thank the State Key Program of Fundamental Research on Rare Earth Functional Materials (G 1998061310), the National Natural Science Foundation of China (29671001, 59872001), and the Doctoral Program Foundation of High Education (99000132) for the financial support.

References

[1] S. Ferrere, B.A. Gregg, J. Am. Chem. Soc. 120 (1998) 843.
[2] H. Lindström, H. Rensmo, S. Sergren, A. Solbrand, S.E. Lindquist, J. Phys. Chem. 100 (1996) 3084.
[3] C. Bechinger, S. Ferrere, A. Zaban, J. Sprague, B.A. Gregg, Nature 383 (1996) 608.
[4] A. Zaban, S. Ferrere, J. Sprague, B.A. Gregg, J. Phys. Chem. B 101 (1997) 55.
[5] S. Das, P.V. Kamat, J. Phys. Chem. B 103 (1999) 209.
[6] A. Solbrand, S.E. Lindquist et al., J. Phys. Chem. B 103 (1999) 1078.

[7] R. Argazzi, C.A. Bignozzi, T.A. Heimer, F.N. Castellano, G.J. Meyer, J. Am. Chem. Soc. 117 (1995) 11815.
[8] B. O'Regen, M. Grätzel, Nature 353 (1991) 737.
[9] P. Bonhe, J.E. Moser, M. Grätzel et al., Chem. Commun. (1996) 1163.
[10] F. Nsch, J.E. Moser, V. Shklover, M. Grätzel, J. Am. Chem. Soc. 118 (1996) 5420.
[11] R. Amadelli, R. Argazzi, C.A. Bignozzi, F. Scandola, J. Am. Chem. Soc. 112 (1990) 7099.
[12] W.S. Xia, C.H. Huang, D.J. Zhou, Langmuir 13 (1997) 80.
[13] W.S. Xia, C.H. Huang, X.Z. Ye, C.P. Luo, L.B. Gan, Z.F. Liu, J. Phys. Chem. 100 (1996) 2244.
[14] A.D. Lang, J. Zhai, C.H. Huang et al., J. Phys. Chem. B 102 (1998) 1424.
[15] W. Zhang, Y.R. Shi, L.B. Gan, C.H. Huang, H.X. Luo, D.G. Wu, N.Q. Li, J. Phys. Chem. B 103 (1999) 675.
[16] D.G. Wu, C.H. Huang, L.B. Gan, W. Zhang, J. Zheng, J. Phys. Chem. B 103 (1999) 4377.
[17] I.R. Girling, N.A. Cade, P.N. Kolinsky, J.D. Earls, G.H. Cross, I.R. Peterson, Thin Solid Films 32 (1985) 101.
[18] T.R. Cheng, C.H. Huang et al., J. Mater. Chem. 7 (1997) 631.
[19] B. O'Regen, J. Moser, M. Anderson, M. Grätzel, J. Phys. Chem. 94 (1990) 8720.
[20] K.J. Donovan, R.V. Sudiwala, E.G. Wilson, Mol. Cryst. 194 (1991) 337.
[21] N. Vlachopoulos, P. Liska, J. Augustynski, M. Grätzel, J. Am. Chem. Soc. 110 (1988) 1216.
[22] A. Hagfeldt, M. Grätzel, Chem. Rev. 95 (1995) 49.
[23] L. Sereno, J.J. Silbeer, L. Otero, M.D.V. Bohorquez, A.L. Moore, T.A. Moore, D. Gust, J. Phys. Chem. 100 (1996) 814.
[24] Y.S. Kim, K. Liang, K.Y. Law, D.G. Whitten, J. Phys. Chem. 98 (1994) 984.